

Supplementary Information

for

Semiconductor Solar Superabsorbers

Yiling Yu², Lujun Huang¹, Linyou Cao^{1,2*}

¹Department of Materials Science and Engineering, North Carolina State University, Raleigh NC 27695;

²Department of Physics, North Carolina State University, Raleigh NC 27695;

* To whom correspondence should be addressed.

Email: lcao2@ncsu.edu

This PDF file includes

Fig. S1-Fig. S3

S1. Calculation for the density of leaky modes including Fig. S4-S7

Fig. S8-Fig.S11

Table S1

Reference S1-S3

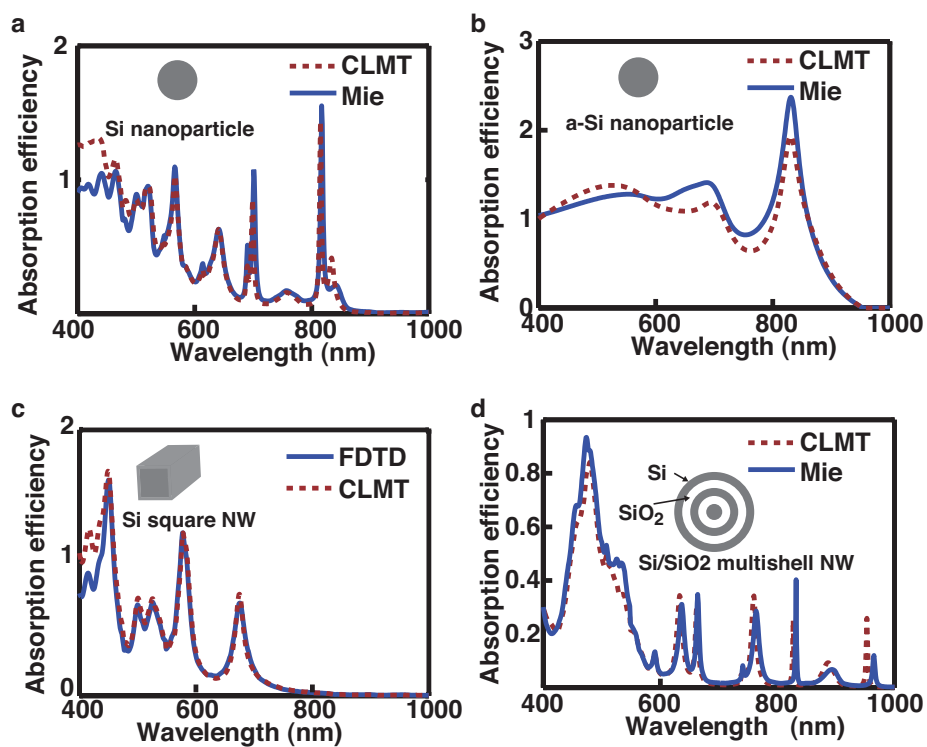


Figure S1. The general validity of CLMT for the analysis of light absorption in semiconductor nanostructures. Calculated spectral light absorption efficiency using the CLMT model (red dashed lines) and well-established analytical or numerical methods (blue solid lines) for (a) Si nanoparticles in radius of 150 nm, (b) a-Si nanoparticles in radius of 150 nm, (c) Si square nanowires in size of 200 nm, and (d) core-multishell Si/SiO₂ nanowires in radius of 300 nm, which equally distributes among the five layers involved. Insets are schematic illustrations for the nanostructures calculated.

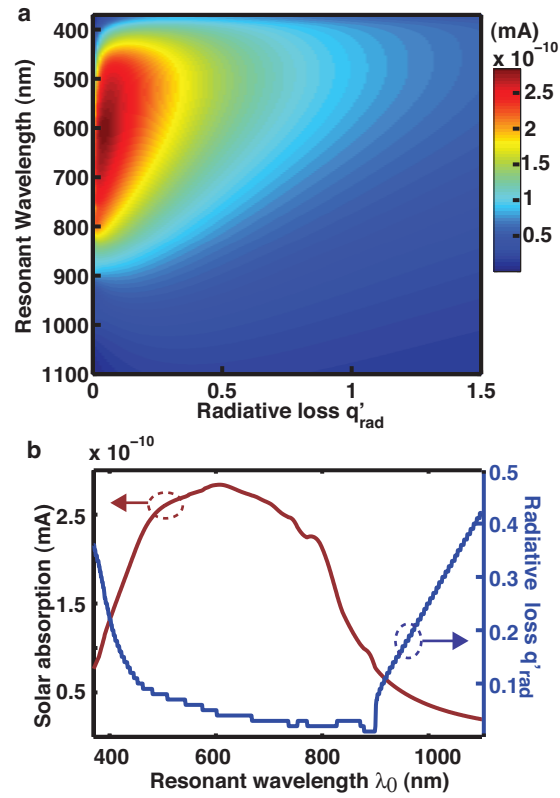


Figure S2. The solar absorption of single leaky modes in 0D Si structures. (a) Calculated solar absorption of single leaky modes in 0D Si structures as a function of radiative loss (horizontal axis) and resonant wavelength (vertical axis). (b) The optimal absorption (red line) and associated radiative loss (blue line) as a function of the resonant wavelength.

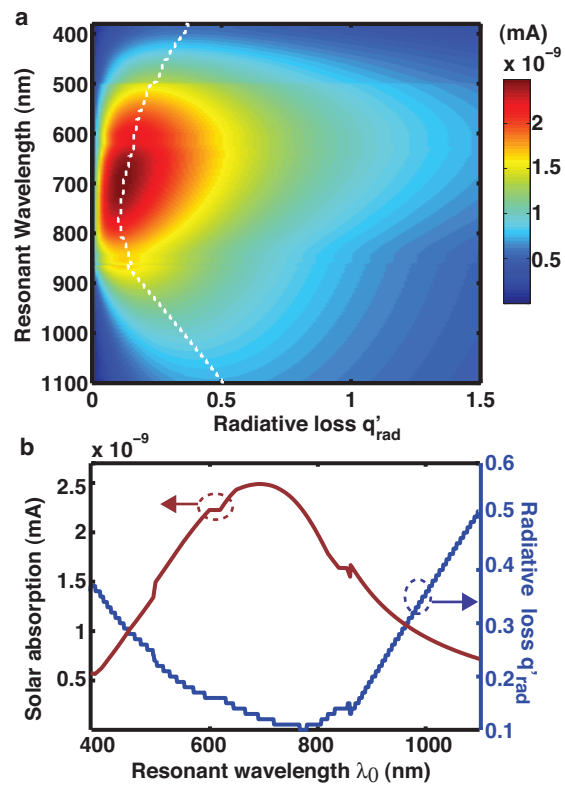


Figure S3. The solar absorption of single leaky modes in 0D CdTe structures. (a) Calculated solar absorption of single leaky modes in 0D CdTe structures as a function of radiative loss (horizontal axis) and resonant wavelength (vertical axis). (b) The optimal absorption (red line) and associated radiative loss (blue line) as a function of the resonant wavelength.

S1. Calculation for the density of leaky modes

For the convenience of mode identification, most of this modal analysis is performed with 1D structures, in which the leaky mode can be identified easier. However, the principle obtained from 1D structures can apply to 0D structures as well.

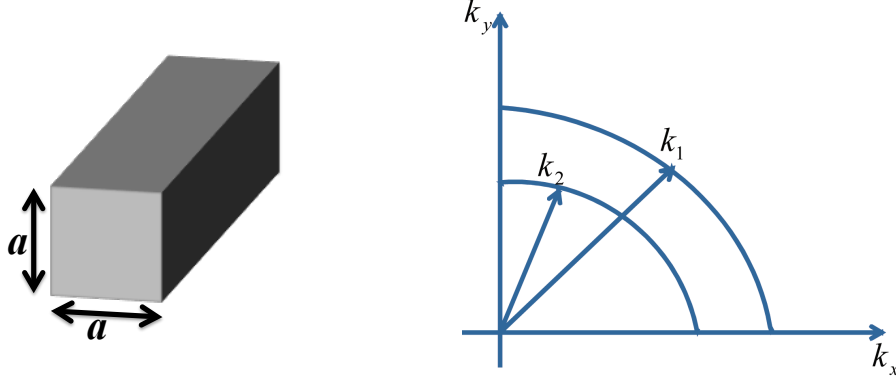


Figure S4. Schematic illustration for 1D square nanowires (left) and for its corresponding mode distribution in k space (right).

we first examine 1D square structure with a refractive index of n as illustrated in Figure S4. We consider modes in wave vector k space. The interspace between neighboring modes in x direction and y direction can be written as $\Delta k_x = \pi/na$ and $\Delta k_y = \pi/na$. The space occupied by one mode is $\Delta k_x \Delta k_y$. For a given space between k_1 and k_2 , $1/4 \cdot \pi(k_1^2 - k_2^2)$, the number of modes can be written as

$$N(\lambda_1, \lambda_2) = \frac{1}{4} \frac{\pi(k_1^2 - k_2^2)}{\Delta k_x \Delta k_y} = \pi \cdot a^2 \cdot n^2 \cdot \left(\frac{1}{\lambda_1^2} - \frac{1}{\lambda_2^2} \right) = \pi A n^2 \left(\frac{1}{\lambda_1^2} - \frac{1}{\lambda_2^2} \right) \quad (\text{S1})$$

Similarly, we also derive the number of modes in 0D cubic structure as

$$N(\lambda_1, \lambda_2) = \frac{1}{8} \frac{4}{3} \frac{\pi(k_1^3 - k_2^3)}{\Delta k_x \Delta k_y \Delta k_z} = \frac{4\pi}{3} \cdot a^3 \cdot n^3 \cdot \left(\frac{1}{\lambda_1^3} - \frac{1}{\lambda_2^3} \right) = \frac{4\pi}{3} V n^3 \left(\frac{1}{\lambda_1^3} - \frac{1}{\lambda_2^3} \right) \quad (\text{S2})$$

From eqs. (S1)-(S2), we can find out the density of modes at given wavelength λ_0 as

$$\text{for 1D,} \quad \rho(\lambda_0) = \frac{dN}{d\lambda} = \frac{2\pi A n^2}{\lambda_0^3} \quad (\text{S3})$$

$$\text{for 0D,} \quad \rho(\lambda_0) = \frac{dN}{d\lambda} = \frac{4\pi V n^3}{\lambda_0^4} \quad (\text{S4})$$

For the case of solar light absorption, we need take into account both transverse magnetic (TM) and transverse electric (TE) modes. Therefore, the density of leaky modes for two polarization are:

for 1D,
$$\rho(\lambda_0) = \frac{4\pi A n^2}{\lambda_0^3} \quad (\text{S5})$$

for 0D,
$$\rho(\lambda_0) = \frac{8\pi V n^3}{\lambda_0^4} \quad (\text{S6})$$

While derived from square and cubic structures, these equations can apply to nanostructures with arbitrary shapes, as illustrated in Figure S5.

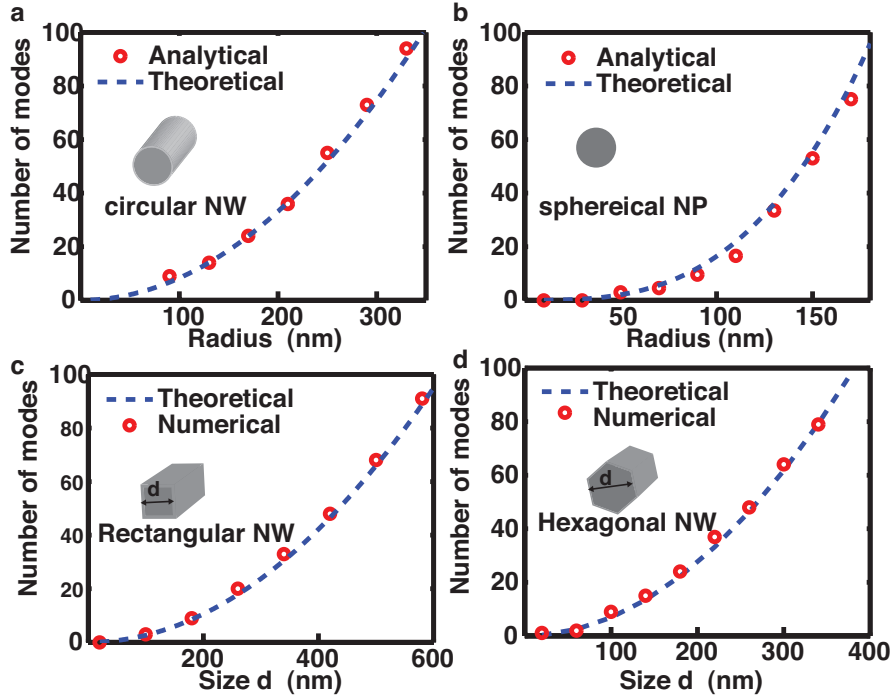


Figure S5. The number of leaky modes calculated using eqs.(S1)-(S2) as a function of size, which is referred as theoretical and plotted as dashed lines. Also plotted is the number of leaky modes directly counted from the eigenvalue calculation of leaky modes using the methods we reported previously.¹⁻³ We can see that eqs.(S1)-(S2) can indeed reasonably describe the number of leaky modes in nanostructures with arbitrary shapes.

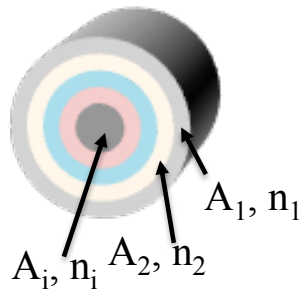


Figure S6. Schematic illustration for heterostructures with absorbing and non-absorbing materials.

We can calculate the number of leaky modes in heterogeneous structures that consist of multiple materials as illustrated Figure S6.

$$\text{for 1D, } N(\lambda_1, \lambda_2) = \pi \cdot (1/\lambda_1^2 - 1/\lambda_2^2) \cdot \sum_i n_i^2 A_i \quad (\text{S7})$$

$$\text{for 0D, } N(\lambda_1, \lambda_2) = \frac{4}{3} \cdot \pi \cdot (1/\lambda_1^3 - 1/\lambda_2^3) \cdot \sum_i n_i^3 V_i \quad (\text{S8})$$

The subscript i here denote different parts of the structure. n_i is the refractive index of the i th part, and A_i , V_i is the corresponding area or volume of the i th part. The validity of these equations is confirmed in Figure S7a, which shows a good consistence between the number of leaky modes calculated using eq. S7 and that counted from eigenvalue calculation¹⁻³. We believe that only those leaky modes mainly related with the absorbing materials may substantially contribute to light absorption.

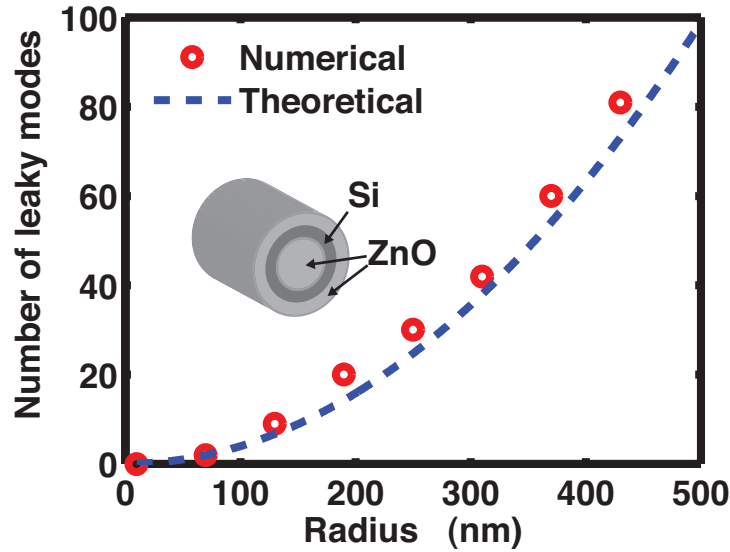


Figure S7. The number of leaky modes for a ZnO/Si/ZnO nanowire, with a constant size ratio of 0.24, 0.36, and 0.4 from inner to outside, calculated using eqs.(S7) as function of the radius, referred as theoretical and plotted as dashed blue line. Also plotted is the number of leaky modes directly counted from the eigenvalue calculation of leaky modes using COMSOL, referred as numerical and plotted as red circle. Inset is a schematic illustration of the NW.

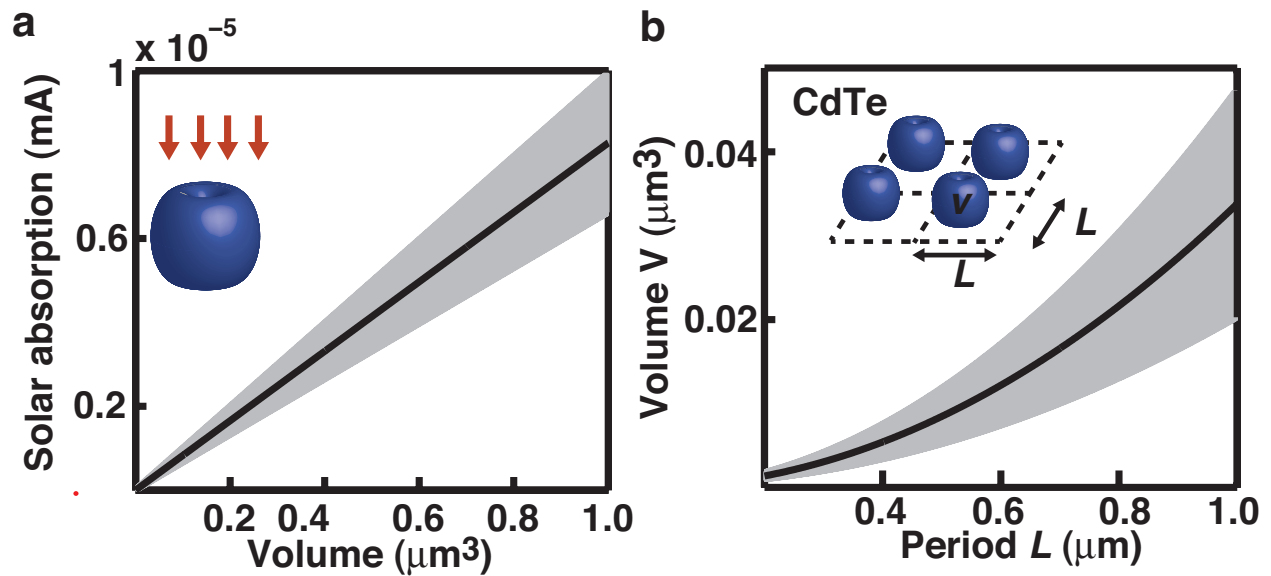


Figure S8. Solar superabsorption in single nanostructures and an array of nanostructures. (a) The maximal solar absorption of single 0D nanostructures in which CdTe is included as the absorbing materials as a function of the volume of CdTe materials. The calculation result includes an estimated 20% error as indicated by the shaded areas. The inset is a schematic illustration for the nanostructure, whose irregular shape is intentionally chosen to illustrate that the structure may have any arbitrary shapes. (b) Solar superabsorption limit of an array of 0D nanostructures. The minimum volume of CdTe materials necessary to absorb >90% of the solar radiation above the band gap is plotted as a function of the period of the array. The inset is a schematic illustration for the nanostructure array.

Table S1. Calculated eigenvalue and radiative loss for the leaky modes in different structures

Mode	Structure 1		Structure 2		Structure 3	
	Eigen value (ka)	Radiative loss (q'_{rad})	Eigen value (ka)	Radiative loss (q'_{rad})	Eigen value (ka)	Radiative loss (q'_{rad})
TM21	0.93 - 0.019i	0.014	1.40 - 0.098i	0.07	1.46 - 0.225i	0.154
TM31	1.26 - 0.003i	0.003	1.85 - 0.044i	0.023	1.72 - 0.187i	0.109
TM41	1.57 - 0.0007i	0.0004	2.28 - 0.019i	0.008	2.71 - 0.179i	0.066
TM61	2.18 - 0.00003i	0.00001	3.07 - 0.003i	0.0008	2.51 - 0.054i	0.023
TE21	1.23 - 0.017i	0.013	2.06 - 0.145i	0.07	1.83 - 0.176i	0.096
TE31	1.55 - 0.003i	0.002	2.58 - 0.094i	0.036	2.08 - 0.240i	0.115

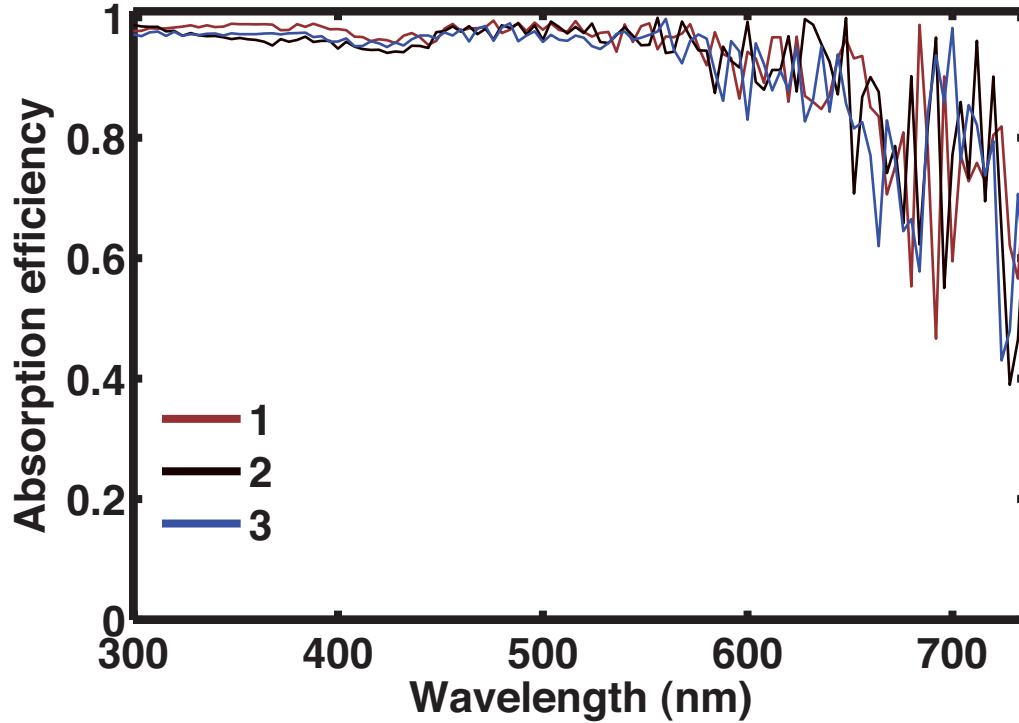


Figure S9. The robustness of the design. The calculated spectral absorption efficiency for the designed nanostructure arrays with a little bit difference in geometrical features. The structure 1 is the one studied in the main text. The detailed geometrical features of the three structures are listed in the following table.

Structure	side	height	a-Si	SiC	ZnO	SiO ₂	Period	Efficiency
1.	180nm	380nm	10nm	30nm	30nm	50nm	540nm	20.69mA/cm ² 90.8%
2.	190nm	390nm	10nm	20nm	40nm	40nm	540nm	20.58mA/cm ² 90.3%
3.	170nm	370nm	10nm	40nm	20nm	20nm	480nm	20.35mA/cm ² 89.3%

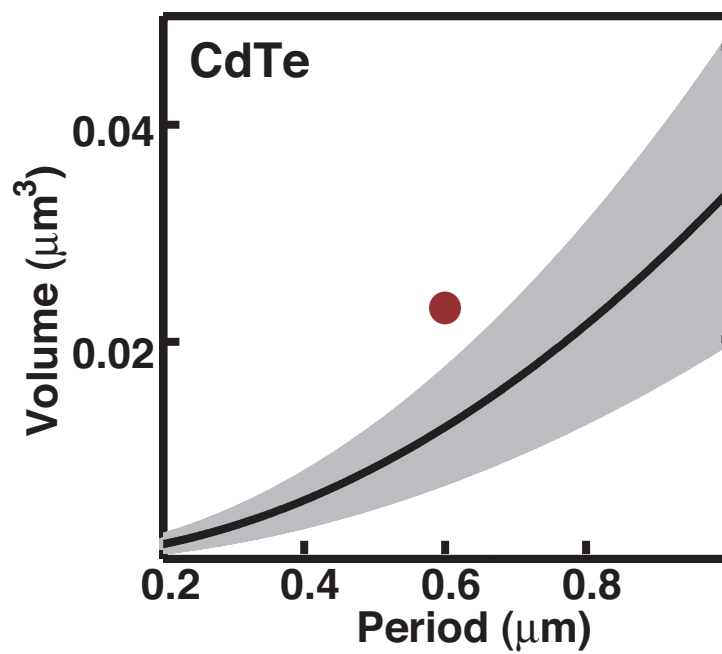


Figure S10. The relationship between the designed structure (the red dot) and the predicted minimum volume for CdTe. The structure is shown in Figure 5d inset in the main text.

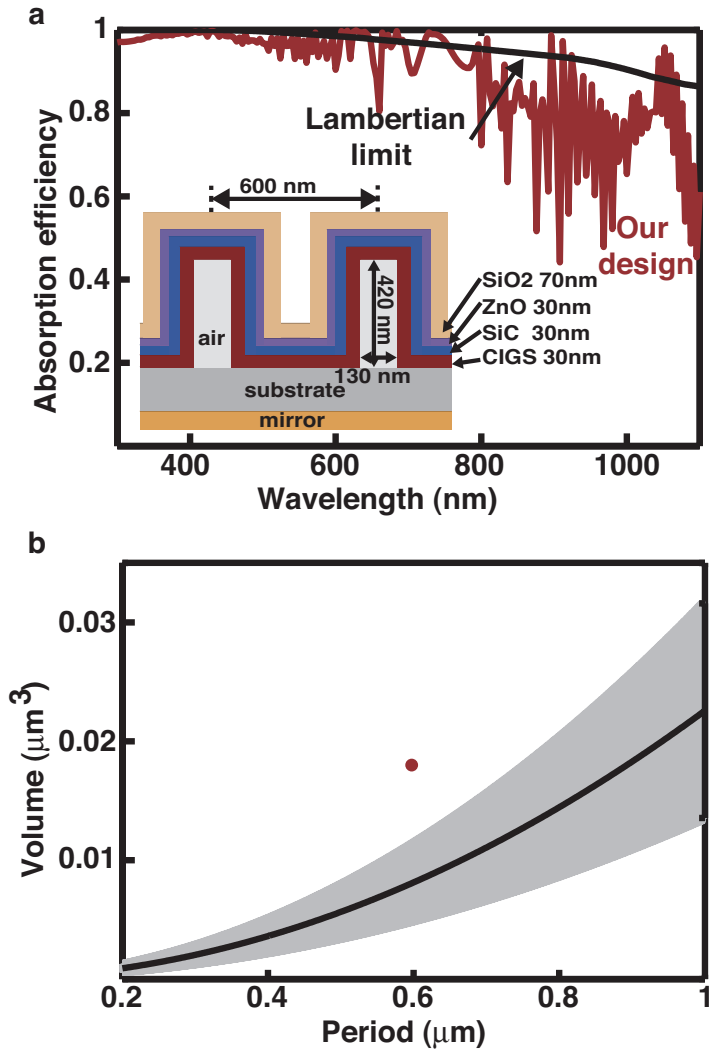


Figure S11. Design of solar superabsorbers for CIGS. (a) The calculated spectral absorption efficiency of a designed structure including 30nm thick CIGS. The Lambertian limit for CIGS with an efficient thickness of 52.5 nm is also given (black). The inset shows the geometry of the designed structure. (b) The relationship between the designed structure (the red dot) and the predicted minimum volume for CIGS.

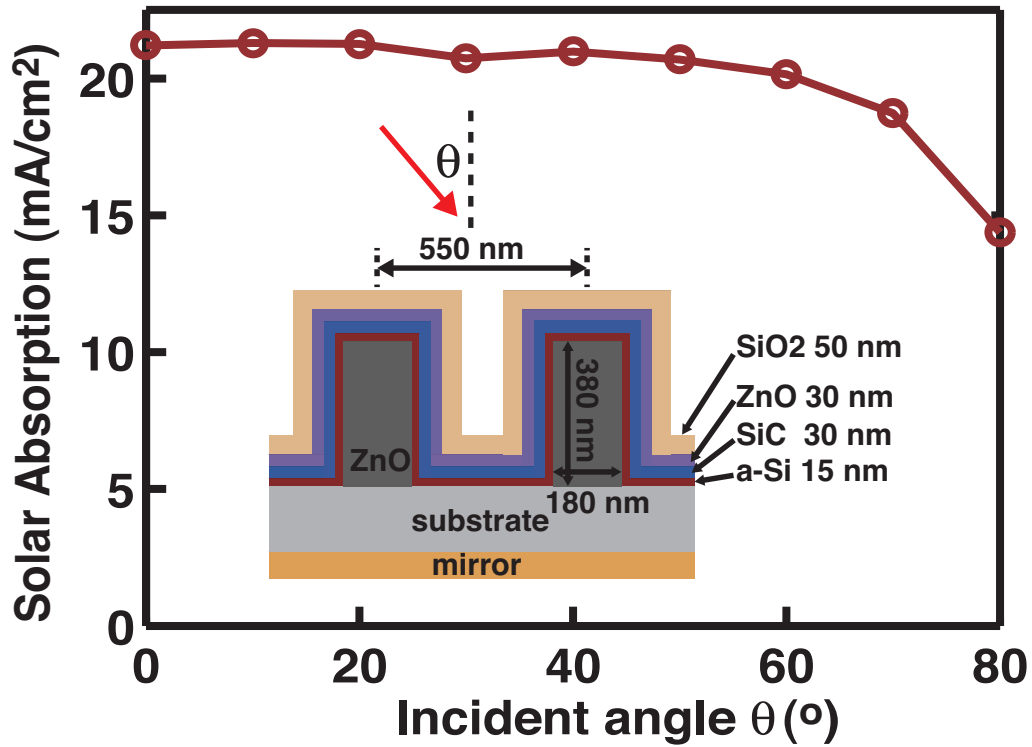


Figure S12 The dependence of the solar absorption on incident angle. The dimension of the structure modeled is given as shown. The definition of the incident angle θ is also schematically illustrated in the figure.

References

- S1 Huang, L. J., Yu, Y. L. & Cao, L. Y. General Modal Properties of Optical Resonances in Subwavelength Nonspherical Dielectric Structures. *Nano Letters* **13**, 3559-3565, (2013).
- S2 Yu, Y. & Cao, L. Coupled leaky mode theory for light absorption in 2D, 1D, and 0D semiconductor nanostructures. *Opt Express* **20**, 13847-13856, (2012).
- S3 Yu, Y. & Cao, L. The phase shift of light scattering at sub-wavelength dielectric structures. *Opt. Express* **21**, 5957-5967, (2013).